Research article

Pan-cancer analysis of the disulfidptosis-related gene *RPN1* and its potential biological function and prognostic significance in gliomas

Yan Zong [a,1], Ankang Zhu [b,1], Peipei Liu [c], Peiji Fu [a], Yinuo Li [a], Shuai Chen [a], Xingcai Gao [b,*]

[a] *Department of Neurology, The Fifth Affiliated Hospital of Zhengzhou University, Zhengzhou University, Zhengzhou, China*
[b] *Department of Thoracic Surgery, The Fifth Affiliated Hospital of Zhengzhou University, Zhengzhou University, Zhengzhou, China*
[c] *Anhui BioX-Vision Biological Technology Co., Ltd., Anhui, China*

ARTICLE INFO

ABSTRACT

Background: Numerous studies have shown a strong correlation between disulfidptosis and various cancers. However, the expression and function of *RPN1*, a crucial gene in disulfidptosis, remain unclear in the context of cancer.
Methods: Gene expression and clinical information on lung adenocarcinoma were obtained from The Cancer Genome Atlas (TCGA) and Genotype-Tissue Expression (GTEx) databases. *RPN1* expression was analyzed using the Timer2.0 and the Human Protein Atlas (HPA) databases. Prognostic significance was assessed using Cox regression analysis and Kaplan–Meier curves. Genetic mutations and methylation levels were examined using the cBioPortal and UALCAN platforms, respectively. The relationship between *RPN1* and tumor mutation burden (TMB) and microsatellite instability (MSI) across different cancer types was analyzed using the Spearman correlation coefficient. The relationship between *RPN1* and immune cell infiltration was analyzed using the Timer2.0 database, whereas variations in drug sensitivity were explored using the CellMiner database. Receiver operating characteristic curves validated *RPN1*'s diagnostic potential in glioma, and its correlation with immune checkpoint inhibitors (ICIs) was assessed using Spearman's correlation coefficient. Single-sample gene set enrichment analysis elucidated a link between *RPN1* and immune cells and pathways. In addition, a nomogram based on *RPN1* was developed to predict patient prognosis. The functional impact of *RPN1* on glioma cells was confirmed using scratch and Transwell assays.
Result: *RPN1* was aberrantly expressed in various cancers and affected patient prognosis. The main mutation type of *RPN1* in the cancer was amplified. *RPN1* exhibited a positive correlation with myeloid-derived suppressor cells, neutrophils, and macrophages, and a negative correlation with CD8$^+$ T cells and hematopoietic stem cells. *RPN1* expression was associated with TMB and MSI in various cancers. The expression of *RPN1* affected drug sensitivity in cancer cells. *RPN1* was positively correlated with multiple ICIs in gliomas. *RPN1* also affected immune cell infiltration into the tumor microenvironment. *RPN1* was an independent prognostic factor for gliomas, and

* Corresponding author. Department of Thoracic Surgery, The Fifth Affiliated Hospital of Zhengzhou University, Zhengzhou University, Zhengzhou, 450000, Henan Province, China.
E-mail address: gxc575788@sina.com (X. Gao).
[1] These authors contributed equally to this work and should be considered co-first authors.

the nomogram demonstrated excellent predictive performance. Interference with *RPN1* expression reduces the migratory and invasive ability of glioma cells.

Conclusion: RPN1 exerts multifaceted effects on different stages of cancer, including immune infiltration, prognosis, and treatment outcomes. *RPN1* expression affects the prognosis and immune microenvironment infiltration in patients with glioma, making *RPN1* a potential target for the treatment of glioma.

1. Introduction

Malignant tumors can arise in various tissues and organs of the human body, leading to a decreased quality of life and poor prognosis in patients with cancer. Overcoming cancer remains a formidable challenge for humanity [1,2]. The onset and progression of tumors involves a multistep, multilevel process encompassing oncogene activation, gene sequence alterations, and aberrant signal transduction [3]. Hence, it is crucial to explore genetics-based cancer treatment approaches.

In recent years, pan-cancer research has gradually become an important approach for exploring the intrinsic mechanisms underlying the onset and progression of malignant tumors. This comprehensive and multifaceted research method has deepened our understanding of cancer and provided strong support for the discovery of preventive and therapeutic methods [4,5]. For specific types of malignant tumors, especially gliomas, one of the most common primary malignant tumors of the central nervous system, pan-cancer research has proven to be particularly important [6]. For example, pan-cancer analysis has identified *CHD5* as a potential biomarker for glioma [7], and pan-cancer research has shown that *NUP37* is a prognostic biomarker associated with the immunosuppressive microenvironment of gliomas [8]. In contrast to other tumors, gliomas not only significantly impact patients' quality of life but also draw attention owing to their high recurrence rate, rapid progression, and lack of effective treatment options [9,10]. Therefore, understanding the pathogenesis of gliomas and identifying novel therapeutic targets are crucial. In addition, in the field of tumor therapy, programmed cell death (PCD) has been a breakthrough in cancer treatment.

Various forms of PCD are closely associated with tumor progression [11]. For instance, ferroptosis, a novel form of PCD that is iron-dependent and distinct from apoptosis, necrosis, and autophagy, plays a dual role in tumorigenesis by promoting tumor growth and inhibiting tumor development [12,13]. Recent research has identified a new type of PCD, disulfidptosis, a rapid death caused by disulfide stress resulting from excessive intracellular cystine accumulation, which leads to abnormal disulfide bonds between actin backbone proteins, causing disintegration of the actin network and cell death [14]. Research has shown that *RPN1*, a core gene associated with disulfidptosis, is aberrantly expressed in various cancers, including melanoma, breast cancer, liver cancer, and bladder cancer. Moreover, high expression of *RPN1* has been linked to hepatocellular carcinoma progression. Recent studies have indicated that targeting *RPN1* may be a viable strategy for bladder cancer treatment. Thus, *RPN1* has great potential in cancer treatment [15–18].

This study analyzed the aberrant expression and mutation status of *RPN1* in cancer and its impact on the prognosis and drug sensitivity of patients with cancer. We further investigated the influence of *RPN1* on the prognosis and immune infiltration status of
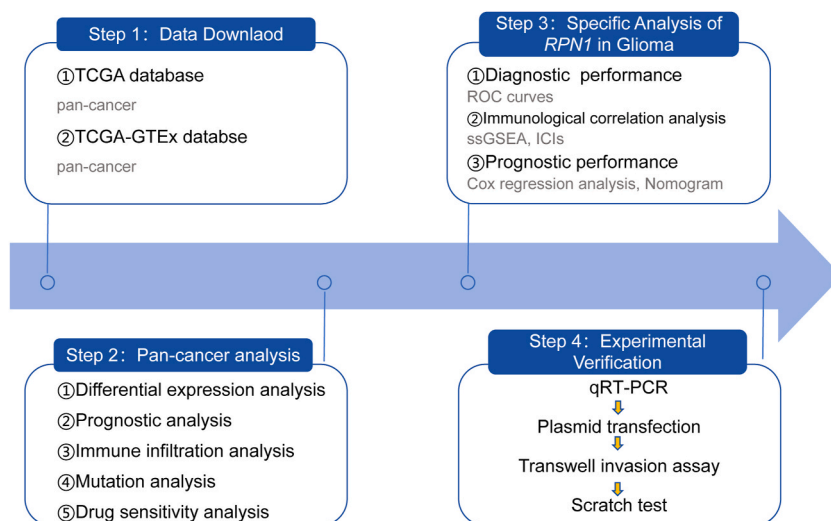
Fig. 1. Overview flowchart of the article. First, we downloaded pan-cancer-related gene expression data and clinical information. In the second step, we conducted a comprehensive analysis of RPN1 expression and gene mutations in pan-cancer using multiple methods, investigating the impact of RPN1 expression on patient prognosis, immune infiltration, and drug sensitivity. In the third step, building upon the pan-cancer analysis in the second step, we observed a higher significance of RPN1 results in gliomas. Therefore, we further analyzed the specific role of RPN1 in gliomas. Finally, we experimentally validated the influence of RPN1 on glioma cells.

patients with glioma and established a nomogram based on *RPN1* expression to predict the prognosis of patients with glioma. Additionally, we validated the effects of *RPN1* on glioma cell function using scratch and Transwell assays.

2. Materials and methods

The research flow of the article is shown in Fig. 1.

2.1. Data download

The gene expression matrix and clinical data for the pan-cancer analysis were sourced from The Cancer Genome Atlas (TCGA) database. Owing to the limited number of normal samples in TCGA database, gene expression matrices and clinical data for normal samples were downloaded from The Genotype-Tissue Expression (GTEx) database.

2.2. Expression of RPN1

The TIMER2.0 database is a tool designed to analyze tumor immune cell infiltration and gene expression. Building upon the foundation of the TCGA database, it offers researchers abundant bioinformatic data pertaining to tumor [19]. We used this database to compare the expression levels of *RPN1* between tumor and normal tissues. The Wilcoxon–Mann–Whitney test was used to calculate the statistical differences in *RPN1* expression among samples from the TCGA database. Owing to the lack of sufficient control samples for certain cancers in the TCGA database, the expression of *RPN1* in both cancer and normal tissues was additionally validated using the TCGA-GTEx dataset.

The Human Protein Atlas (HPA) database provides extensive information on human proteins at both tissue and cellular levels, including various data sources, such as immunohistochemistry (IHC), immunofluorescence, mass spectrometry, and cellular imaging [20]. We obtained IHC results for *RPN1* in multiple cancers and their corresponding normal tissues from this database.

2.3. Survival analysis

We evaluated the role of *RPN1* in overall survival (OS) across multiple cancers using univariate Cox regression analysis [21], in which the hazard ratio (HR) was used to assess the outcomes. We then divided the patients into two groups (high- and low-expression groups) based on the median value of *RPN1* expression. The effect of *RPN1* expression on patient prognosis was compared using Kaplan–Meier survival curves [22].

2.4. Immune infiltration of RPN1 in pan-cancer

We determined the correlation between *RPN1* expression in tumor tissues and various immune cells from the TIMER 2.0 database [23]. This database integrates multiple analysis tools (XCELL, QUANTISEQ, TIMER, TIDE, CIBERSORT, CIBERSORT-ABS, EPIC, and MCPcounter) and uses partial Spearman correlation analysis to examine the relationship between *RPN1* and immune cells. Explanations of these tools are provided in Table 1.

2.5. Gene enrichment analysis

GEPIA is an online platform for the rapid analysis and visualization of gene expression data and provides information about genes of interest [24]. From this database, we identified the top 100 genes that were most strongly correlated with *RPN1* in cancer. Gene Oncology (GO) and Kyoto Encyclopedia of Genomics (KEGG) analyses were performed for these genes. The results of GO analyses consisted of three categories: cellular components (CC), biological pathways (BP), and molecular functions (MF). $p < 0.05$ was considered statistically significant, and the results were visualized using the R package "ggplot2" to explore the potential functions of *RPN1*.

Table 1
Interpretation of multiple immune infiltration calculation tools.

Tools	Interpretation
XCELL	A computational tool for estimating the abundance of immune cell types based on gene expression data.
QUANTISEQ	A tool employing sophisticated algorithms to infer the relative abundance of different immune cell types within tumor tissues.
TIMER	The tool is based on gene expression data to estimate the relative abundance of various immune cell types within tumor tissues.
TIDE	A tool for predicting the responsiveness of immune checkpoint inhibitors in tumors.
CIBERSORT	A computational tool used to estimate the abundance of various cell types in complex cell mixtures.
CIBERSORT-ABS	An extended version of CIBERSORT used to estimate the absolute abundance of cell types rather than relative abundance.
EPIC	A computational tool used to estimate the abundance of immune cell types, particularly suitable for tumor samples.
MCPcounter	A computational tool used to assess the abundance of different cell types in the tumor microenvironment from gene expression data.

2.6. Mutations and methylation levels

UALCAN is an online platform for analyzing and visualizing TCGA tumor data, including gene expression and methylation information [25]. We used this platform to compare the methylation status of *RPN1* between normal and tumor samples.

Additionally, cBioPortal is an open platform for the interactive exploration of large-scale cancer genomic data [26]. We used this platform to analyze the genetic mutation status of *RPN1* in tumors. According to a study conducted by *Bonneville* et al., we obtained the microsatellite instability (MSI) scores for tumor samples from TCGA database [27]. In addition, we calculated the tumor mutation burden (TMB) for each tumor using the "TMB" function in the R package "maftools." Subsequently, we statistically analyzed and visualized the results using the R package "fmsb."

2.7. Drug sensitivity

CellMiner is a cancer cell line-based database that provides extensive molecular characterization and drug response data for various cancer cell lines [28]. We obtained drug sensitivity data from this database and analyzed the differences in sensitivity between *RPN1* and various drugs using Spearman's correlation coefficients. A correlation coefficient (cor) greater than 0.3 was considered significant. We visualized the results using the R package "ggplot2."

2.8. Clinical value of RPN1 for gliomas

With significant results for gliomas in several pan-cancer studies, we investigated the role of *RPN1* in the diagnosis, progression, and prognosis of gliomas. The training cohort (TCGA-GBMLGG) comprised 706 samples, including five non-tumor samples. Of these, 699 samples with survival data were used for the prognosis-related analyses. Of these 699 samples, 427 were survivors (censored samples) and 272 were deceased. The validation cohort (TCGA-GTEx) contained 1846 samples, of which 689 were glioma samples and 1157 were normal samples.

We validated the diagnostic performance of *RPN1* by plotting the receiver operating characteristic curves (ROC) of the training and validation cohorts using the R package "pROC." Univariate and multivariate Cox regression analyses were performed to confirm whether *RPN1* was an independent prognostic factor for gliomas. An *RPN1*-based nomogram was constructed to predict patients' survival at 1, 2, and 3 years using "rms" (https://cran.r-project.org/package=rms) and "survival" (https://cran.r-project.org/package=survival) package, and calibration curves were established to verify its performance [29].

2.9. Immune-related functional analysis of RPN1 in gliomas

The association of *RPN1* with several common immune checkpoint inhibitors (ICIs) was calculated using the Spearman correlation coefficient, and the results were plotted as a chordal plot using the R package "circlize." Gene sets of immune cells and immune-related functions were downloaded from the MSigDB database. (https://www.gsea-msigdb.org/gsea/msigdb). The enrichment scores for immune-infiltrating cells and immune-related functions were analyzed in TCGA-GBMLGG samples using a single-sample genome enrichment analysis (ssGSEA) algorithm.

2.10. Cell culture and quantitative reverse transcription-polymerase chain reaction (qRT-PCR)

HA-1800 (normal human astrocytes) and U-87 (human glioma astrocytoma cells) cells were procured from Wuhan Punuo Sai Life Science Co., Ltd. and cultured in DMEM (Gibco, USA) supplemented with 10 mL of fetal bovine serum (FBS). Total RNA was extracted using the TRIzol reagent (Sebasun, China), and cDNA was synthesized using a reverse transcription kit (Toyobo Biotechnology Co., Ltd., Shanghai, China). The mRNA expression levels were detected on a PCR instrument under the following conditions: 95 °C for 20 s, 55 °C for 20 s, and 72 °C for 20 s for 40 cycles. The relative gene expression levels were calculated using the $2^{-\Delta\Delta CT}$ method with GAPDH as the internal reference. Detailed primer sequences are listed in Table 2.

2.11. Plasmid transfection experiment

U87 cells in the logarithmic growth phase were seeded in six-well plates at a density of 1×10^5 cells/well and cultured until confluency reached 80 % or higher. The cells were then divided into three groups: (1) blank group: untreated U87 cells. (2) NC group: The negative control plasmid (NC plasmid) was transfected into U87 cells using a transfection reagent (Lipofectamine 2000). (3)

Table 2
Primer sequences used in PCR experiments.

Gene	Primer sequence (5′–3′)	
GAPDH	Forward	TCAGCAATGCCTCCTGCAC
	Reverse	TCTGGGTGGCAGTGATGGC
C10orf55	Forward	GGACCTACTGGATTATGGG
	Reverse	GATGGTCTTAAAAGAACGGA

si*RPN1* group: The siRNA plasmid was transfected into U87 cells using a transfection reagent. The sequences of the NC plasmid and si*RPN1* plasmid are listed in Table 3. Subsequent experiments were performed using cells from all three groups.

2.12. Scratch assays and transwell invasion assays

ECM gel matrix (BD Biosciences, USA) was diluted to 1 mg/mL in PBS and applied at 50 μL per well onto Transwell chamber membranes. Cells were seeded at a density of 5.0×10^5 cells/mL in 200 μL per well in the upper chamber, while 500 μL of culture medium containing 10 % FBS was added to the lower chamber. After 48 h of incubation, the membrane in the bottom chamber was fixed with paraformaldehyde and stained with crystal violet. Subsequently, the cells were counted under a 100x microscope (the number of cells in the upper, lower, left, right, and middle regions and the average were calculated).

Cells were seeded at a 5×10^5 cells/mL density per well in six-well plates. After reaching confluence, a straight line was scratched vertically across the well surface using a sterile pipette tip, followed by the addition of serum-free culture medium. The cells were then incubated at 37 °C with 5 % CO_2, and images were captured at 24 and 48 h.

2.13. Statistical analysis

In this study, for continuous variable data that followed a normal distribution, we employed the *t*-test (Student's t-test) to analyze their correlations. For data that did not meet the normal distribution criteria or for two independent samples, the Wilcoxon–Mann–Whitney test was utilized. Additionally, the Kruskal–Wallis test was used to examine correlations among more than two independent samples. The Spearman's correlation coefficient was used to measure the strength and direction of the nonlinear relationships between two variables. A *p*-value below 0.05 was considered statistically significant. "*," "**," and "***" represent $p < 0.05$, $p < 0.01$, and $p < 0.001$, respectively.

3. Results

3.1. Expression of RPN1 in pan-cancer

Based on *RPN1* expression data from TCGA and TCGA-GTEx databases, compared with normal tissues, *RPN1* expression levels were elevated in BLCA, BRCA, CESC, CHOL, COAD, ESCA, HNSC, LIHC, LUAD, LUSC, READ, STAD, UCEC, ACC, DLBC, GBMLGG, LAML, OV, SKCM, TGCT, THYM, and UCS tissues. Conversely, decreased expression of *RPN1* was observed in KICH and THCA (Fig. 2A–K) (abbreviations and full names are listed in Table 4).

The HPA database suggests that RPN1 is expressed at high levels in normal tissues, such as the gastrointestinal tract, pancreas, and testis, and at low levels in muscles and soft tissues (Supplementary Fig. 1A). Simultaneously, RPN1 is also highly expressed in a variety of cancers, such as myeloma, ovarian cancer, skin cancer, kidney cancer, and bladder cancer (Supplementary Fig. 1B). In addition, we obtained IHC results for RPN1 in selected cancers and their corresponding normal tissues from this database. These results also demonstrate the high expression of RPN1 in LUAD, GBMLGG, COADREAD, HNSC, KIRC, LIHC, CESC, OV, and UCEC, in agreement with our previous findings (Fig. 3A–I).

3.2. Survival analysis

Univariate Cox regression analysis revealed that *RPN1* was an adverse prognostic factor (HR > 1) for multiple cancer types, including ACC, BLCA, GBMLGG, KICH, LIHC, and PAAD. Conversely, *RPN1* was a favorable prognostic factor (HR < 1) for DLBC and THYM (Fig. 4A). Furthermore, Kaplan–Meier survival curves demonstrated that elevated expression of *RPN1* was associated with poor prognosis in patients with HNSC, LUAD, ACC, BLCA, GBMLGG, KICH, LIHC, and PAAD. In contrast, it was correlated with prolonged survival in patients with KIRC, READ, and THYM (Fig. 4B-L). The Kaplan–Meier survival curves for other cancers are not shown because their *p*-values were >0.05. These findings were highly consistent with the univariate Cox regression analysis results.

3.3. Correlation between RPN1 and immune cell infiltration

Cancer is typically accompanied by widespread immune system dysfunction, and tumor progression is closely associated with immune cell infiltration [30]. Therefore, investigating the correlation between *RPN1* and immune cell infiltration in tumor tissues is critical to understand the immune regulatory mechanisms of cancer and discover potential therapeutic approaches. Our study found

Table 3
Gene sequences of transfected plasmids.

siRNA	Gene sequence (5′–3′)	
RPN1-siRNA	Forward	ACAUCUUUGUGUUUUUUGAACAAAG
	Reverse	AGUGCGCUCGGCUUGCUUGUUUUU
SiRNA-NC	Forward	UUCUCCGAACGUGUCACGUTT
	Reverse	ACGUGACACGUUCGGAGAATT
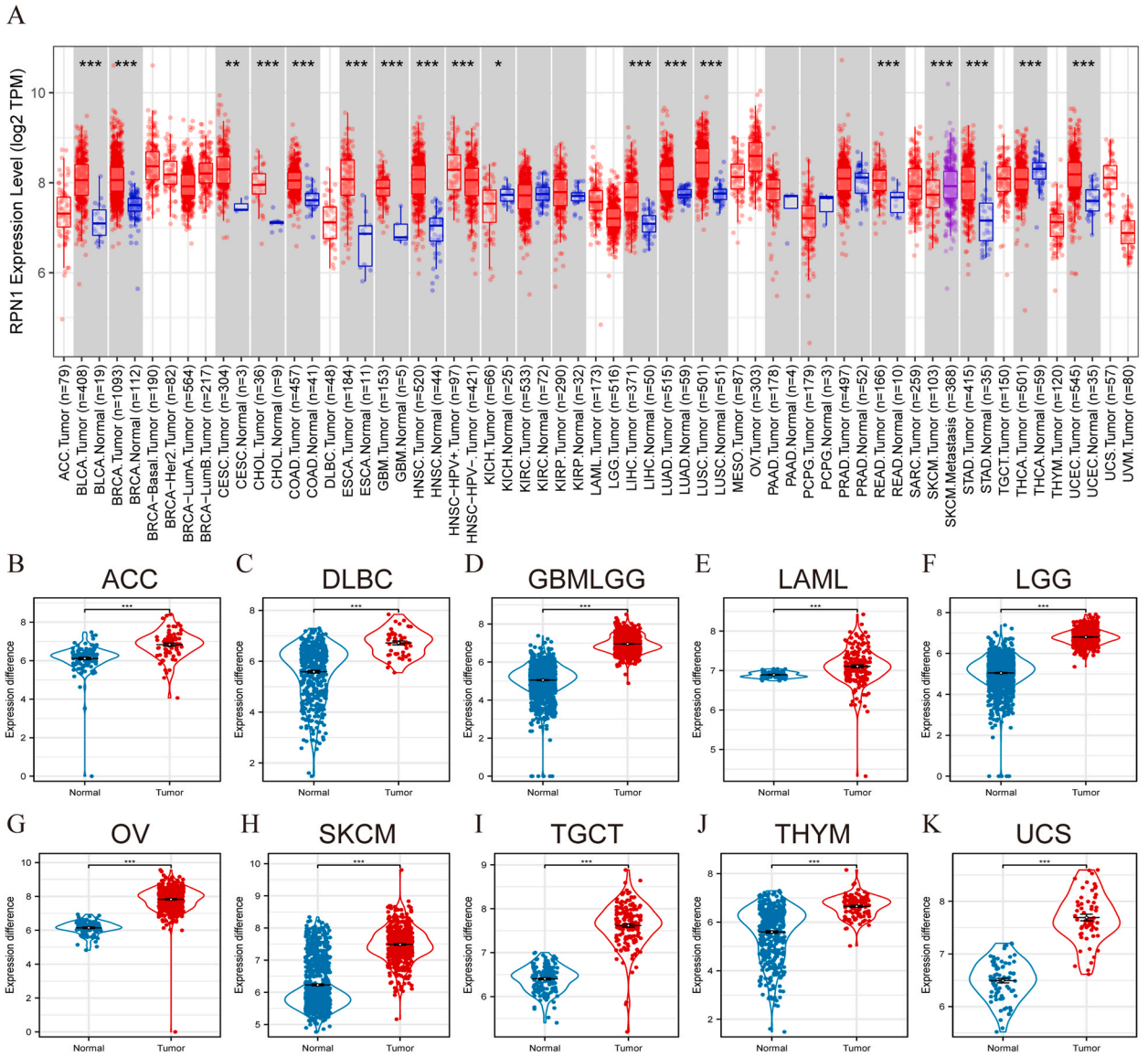
Fig. 2. Expression levels of *RPN1* in pan-cancer tissues. (A) Expression of *RPN1* in cancer and normal tissues in the Timer2.0 database. (B–K) Comparison of the expression difference of *RPN1* in normal and tumor tissues. "*" denotes $p < 0.05$, "**" denotes $p < 0.01$, "***" denotes $p < 0.001$.

that *RPN1* was positively correlated with myeloid-derived suppressor cells (MDSCs) (Fig. 5A), neutrophils (Fig. 5B), and macrophages (Fig. 5C), but negatively correlated with CD8$^+$ T cells (Fig. 5D) and hematopoietic stem cells (HSCs) (Fig. 5E). Additionally, the correlation of *RPN1* with regulatory T cells (Tregs), cancer-associated fibroblasts (CAFs), CD4$^+$ T cells, myeloid dendritic cells (mDCs), natural killer (NK) cells, and endothelial cells was diverse (Fig. 5F–K), which may be attributed to heterogeneity among different types of tumors and algorithmic differences in the immune calculation tools used. The significance of these findings is elaborated on in the Discussion section.

3.4. Enrichment analysis

From the GEPIA platform, we obtained the top 100 genes that were the most closely associated with *RPN1* in cancer (Supplementary Table 1). GO analysis of these 100 genes indicated that *RPN1* was predominantly enriched in endoplasmic reticulum-related functions (such as stress response and vesicle transport), glycoprotein metabolism, and enzyme-related functions (including oxidoreductase and protein disulfide isomerase activity) (Supplementary Figs. 2A–C). Furthermore, KEGG analysis suggested that these molecules were mainly involved in protein export, protein processing in the endoplasmic reticulum, various forms of N-glycan biosynthesis, and *Vibrio cholerae* infection (Supplementary Fig. 2D). Thus, *RPN1* plays a role in critical cellular processes, such as

Table 4
Abbreviations and corresponding full names of tumors.

| TCGA	TUMOR	TCGA	TUMOR
ACC	Adrenocortical carcinoma	MESO	Mesothelioma
BLCA	Bladder Urothelial Carcinoma	OSCC	Oral squamous cell carcinoma
BRCA	Breast invasive carcinoma	OV	Ovarian serous cystadenocarcinoma
CESC	Cervical squamous cell carcinoma and endocervical adenocarcinoma	PAAD	Pancreatic adenocarcinoma
CHOL	Cholangiocarcinoma	PCPG	Pheochromocytoma and Paraganglioma
COAD	Colon adenocarcinoma	COADREAD	Colon and rectum adenocarcinoma
DLBC	Lymphoid neoplasm diffuse large B-cell Lymphoma	READ	Rectum adenocarcinoma
ESCA	Esophageal carcinoma	SARC	Sarcoma
GBMLGG	Glioma	SKCM	Skin cutaneous melanoma
HNSC	Head and neck squamous cell carcinoma	STAD	Stomach adenocarcinoma
KICH	Kidney chromophobe	STES	Stomach and esophageal carcinoma
KIRC	Kidney renal clear cell carcinoma	TGCT	Testicular germ cell tumors
KIRP	Kidney renal papillary cell carcinoma	THCA	Thyroid carcinoma
LAML	Acute myeloid leukemia	THYM	Thymoma
LIHC	Liver hepatocellular carcinoma	UCEC	Uterine corpus endometrial Carcinoma
LUAD	Lung adenocarcinoma	UCS	Uterine carcinosarcoma
LUSC	Lung squamous cell carcinoma	UVM	Uveal melanoma
PRAD	Prostate adenocarcinoma		
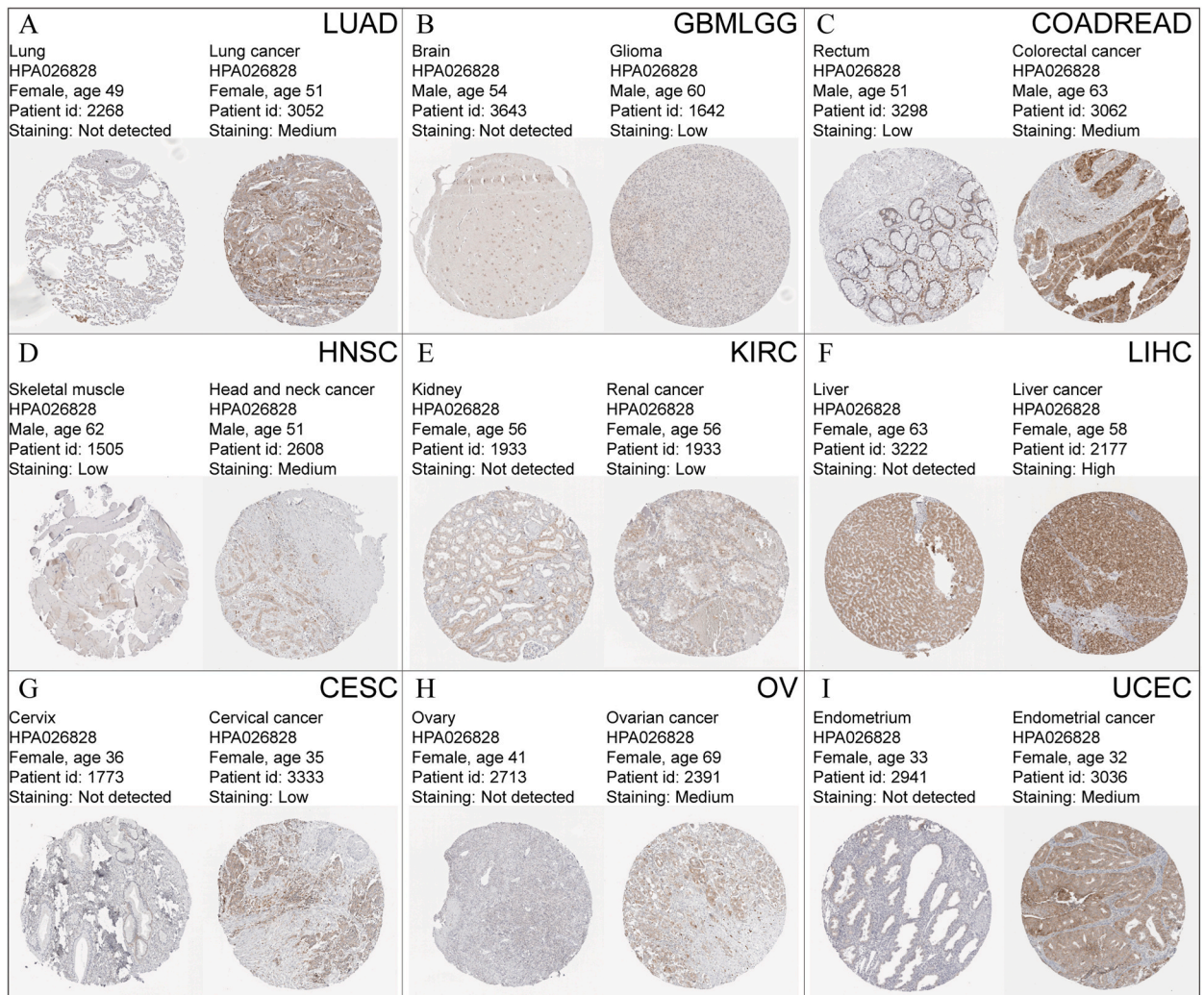
Fig. 3. IHC images of *RPN1* protein expression levels in normal and corresponding tumor tissues. (A–I) *RPN1* expression was higher in LUAD, GBMLGG, COADREAD, HNSC, KIRC, LIHC, CESC, OV, and UCEC.

A

Cancer	HR (95% CI)		P value
ACC	2.577 (1.448 – 4.585)		0.001
PCPG	0.860 (0.276 – 2.679)		0.795
BLCA	1.369 (1.049 – 1.787)		0.021
BRCA	0.962 (0.691 – 1.339)		0.82
CESC	1.054 (0.645 – 1.722)		0.834
CHOL	1.179 (0.461 – 3.015)		0.73
COAD	1.232 (0.800 – 1.898)		0.344
READ	0.549 (0.222 – 1.357)		0.194
LAML	1.158 (0.769 – 1.742)		0.483
DLBC	0.067 (0.008 – 0.589)		0.015
ESCA	1.131 (0.740 – 1.730)		0.569
GBMLGG	5.603 (4.367 – 7.189)		< 0.001
HNSC	1.281 (0.995 – 1.650)		0.054
KIRC	0.832 (0.625 – 1.107)		0.206
KICH	6.548 (1.610 – 26.627)		0.009
KIRP	1.465 (0.837 – 2.566)		0.182
LICH	1.982 (1.394 – 2.817)		< 0.001
LUAD	1.160 (0.866 – 1.554)		0.32
LUSC	1.038 (0.798 – 1.351)		0.781
OV	0.977 (0.758 – 1.259)		0.856
PAAD	1.996 (1.216 – 3.278)		0.006
PRAD	1.345 (0.389 – 4.646)		0.64
SKCM	0.911 (0.716 – 1.160)		0.45
STAD	0.964 (0.732 – 1.270)		0.793
TGCT	2.086 (0.165 – 26.431)		0.57
THCA	1.404 (0.491 – 4.016)		0.527
THYM	0.103 (0.019 – 0.565)		0.009
UCEC	1.146 (0.808 – 1.625)		0.444
UCS	0.721 (0.313 – 1.659)		0.441
UVM	0.780 (0.289 – 2.103)		0.623
OSCC	1.325 (0.987 – 1.778)		0.061
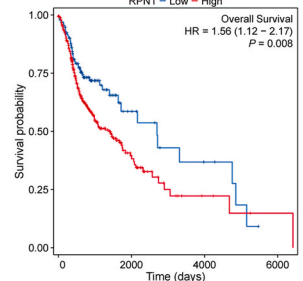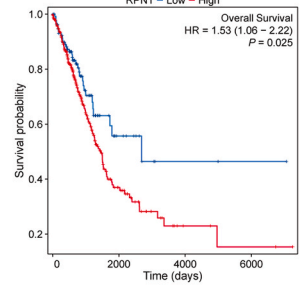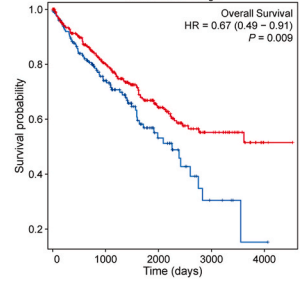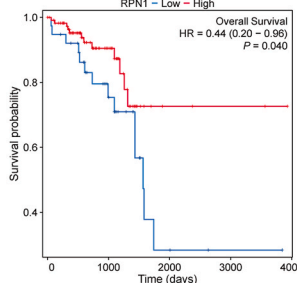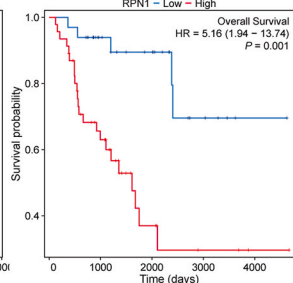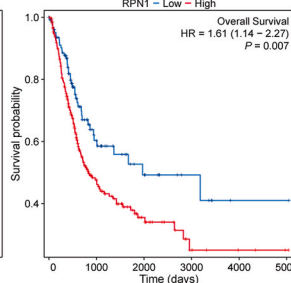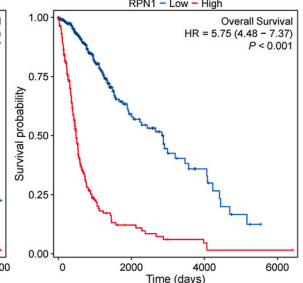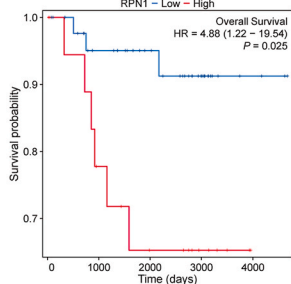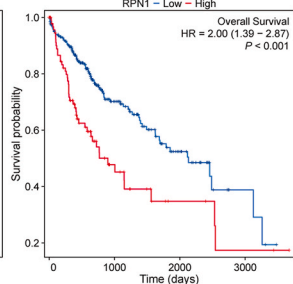
(caption on next page)

Fig. 4. Survival analysis of *RPN1* in pan-cancer. (A) Forest plot of the correlation between *RPN1* expression and OS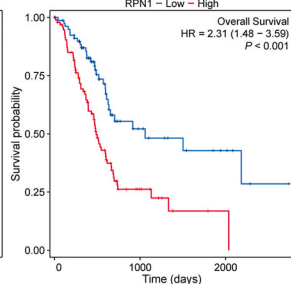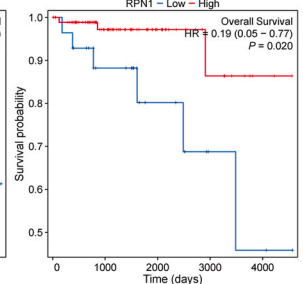 in pan-cancer tissues. HR > 1 represents that *RPN1* is a poor prognostic factor for this tumor, while HR < 1 represents that *RPN1* is a favorable prognostic factor. (B–C) *RPN1* expression decreased the survival of patients with HNSC and LUAD. (D–E) *RPN1* expression increased the survival rate of patients with KIRC and READ. (F–L) Kaplan–Meier curves showed that *RPN1* expression on ACC, BLCA, GBMLGG, KICH, LIHC, and PAAD decreased survival, while expression on THYM increased survival.
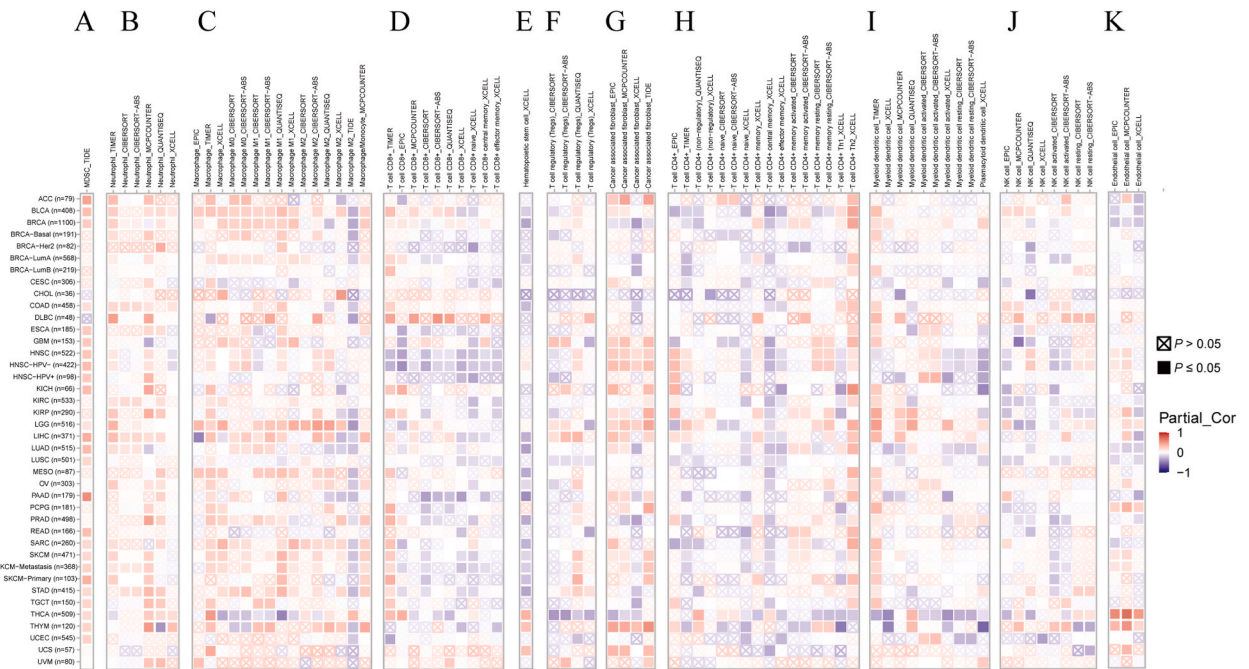
Fig. 5. Effects of *RPN1* expression on immune cells. (A–K) Relationships between *RPN1* expression and immune infiltration of MDSCs, neutrophils, macrophages, CD8$^+$ T cells, hematopoietic stem cells, Tregs, CD4$^+$ T cells, DC cells, NK cells, and endothelial cells were analyzed using the TIMER 2.0 database. Positive correlations are shown in red, negative correlations in blue, and $p < 0.05$ was considered significant.

protein glycosylation, endoplasmic reticulum function, protein export, and protein metabolism. These findings deepen our understanding of *RPN1*'s function in cellular activities and pave the way for future cancer research and treatments.

3.5. Genetic alterations of RPN1 in pan-cancer

Gene mutations are essential for the occurrence and progression of cancer. Therefore, we explored the level of gene mutations of *RPN1* in different types of cancer. The results indicated that the mutation level of *RPN1* was the highest in cervical cancer, followed by endometrial, non-small cell lung, ovarian epithelial, and head and neck cancers (Fig. 6A). These were primarily caused by gene amplification and missense mutations (Fig. 6B–D). Following *RPN1* mutations, there were significant increases in the mutation rates of *SULT1D1P*, *LRRTM4-AS1*, *LINC01851*, *SNAR-H*, *LINC01565*, *DNAJB8*, *PLXND1*, *DNAJB8-AS1*, *CFAP92*, and *PLXNA1* (Fig. 6C). This suggests that these gene mutations may be involved in driving specific cellular signaling pathways of tumor occurrence, indicating the involvement of *RPN1* in the progression of tumors with these genes. This is crucial for understanding the process of cancer occurrence and development and related carcinogenic mechanisms.

Studies have shown that DNA promoter methylation is closely related to gene transcription and directly correlated with the occurrence and development of tumors. Characteristic methylation sites play a crucial role in the diagnosis, classification, prognosis, and treating tumors [31]. Therefore, we compared the methylation levels of *RPN1* in normal tissues and the corresponding tumor samples using the UALCAN platform. Fig. 6E–S shows results with statistical differences (p < 0.05), indicating a significant decrease in the methylation levels of *RPN1* in tumor tissues, such as KIRC, ESCA, SARC, LUAD, READ, KIRP, UCEC, LIHC, BLCA, PRAD, TGCT, LUSC, HNSC, COAD, and BRCA. This suggests that the expression of *RPN1* in cancer may be influenced by changes in methylation levels, thus affecting the biological behavior of tumor cells.

3.6. Relationship among RPN1, TMB, and MSI

Currently, TMB and MSI are receiving increasing attention in tumor therapy. Research indicates that TMB and MSI may serve as potential indicators of immune response [32,33]. High TMB and MSI levels tended to result in improved immune reactivity [34]. We
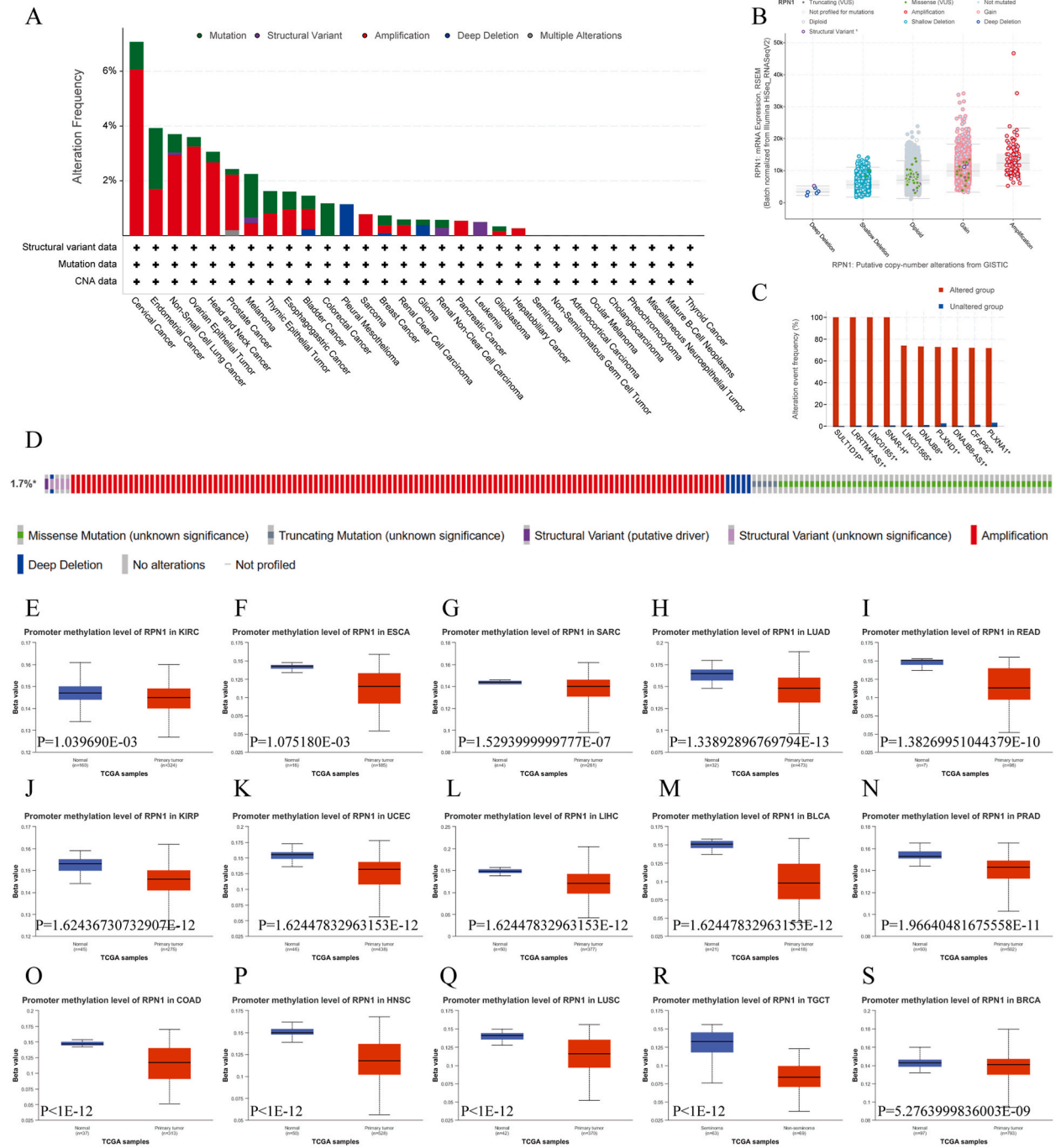
Fig. 6. Genetic alterations in *RPN1*. (A) Analysis of *RPN1* gene alterations in human tumor tissues. (B) Types of gene alterations in *RPN1*. (C) Mutation rates of relevant genes in the *RPN1* gene alteration and unaltered groups. (D) Overview of the types of *RPN1* gene alterations. (E–S) A study using UALCAN software to analyze differences in promoter methylation of the *RPN1* gene in normal and primary tumor tissues.

then explored the association among *RPN1* expression, TMB, and MSI in pan-cancers. Fig. 7A shows that TMB was positively associated with six cancers: GBMLGG (cor = 0.089, p = 0.023), LUAD (cor = 0.19, p < 0.001), COAD (cor = 0.154, p = 0.009), BRCA (cor = 0.083, p = 0.009), SARC (cor = 0.165, p = 0.011), and STAD (cor = 0.138, p = 0.005). The results of the correlation analyses for all cancers are presented in Supplementary Table 2. We observed a correlation between *RPN1* and MSI. We found a significant correlation with nine tumors; CESC (cor = 0. 127, p = 0.027), COAD (cor = 0.192, p = 0.001), SARC (cor = 0.133, p = 0.034), STAD (cor = 0.152, p = 0.002), READ (cor = 0.222, p = 0.036), and BLCA (cor = 0.107, p = 0.032) showed a positive correlation, while GBMLGG (cor = −0. 374, p < 0.001), PRAD (cor = −0.154, p < 0.001), and THCA (cor = −0.175, p < 0.001) showed a negative correlation (Fig. 7B–Supplementary
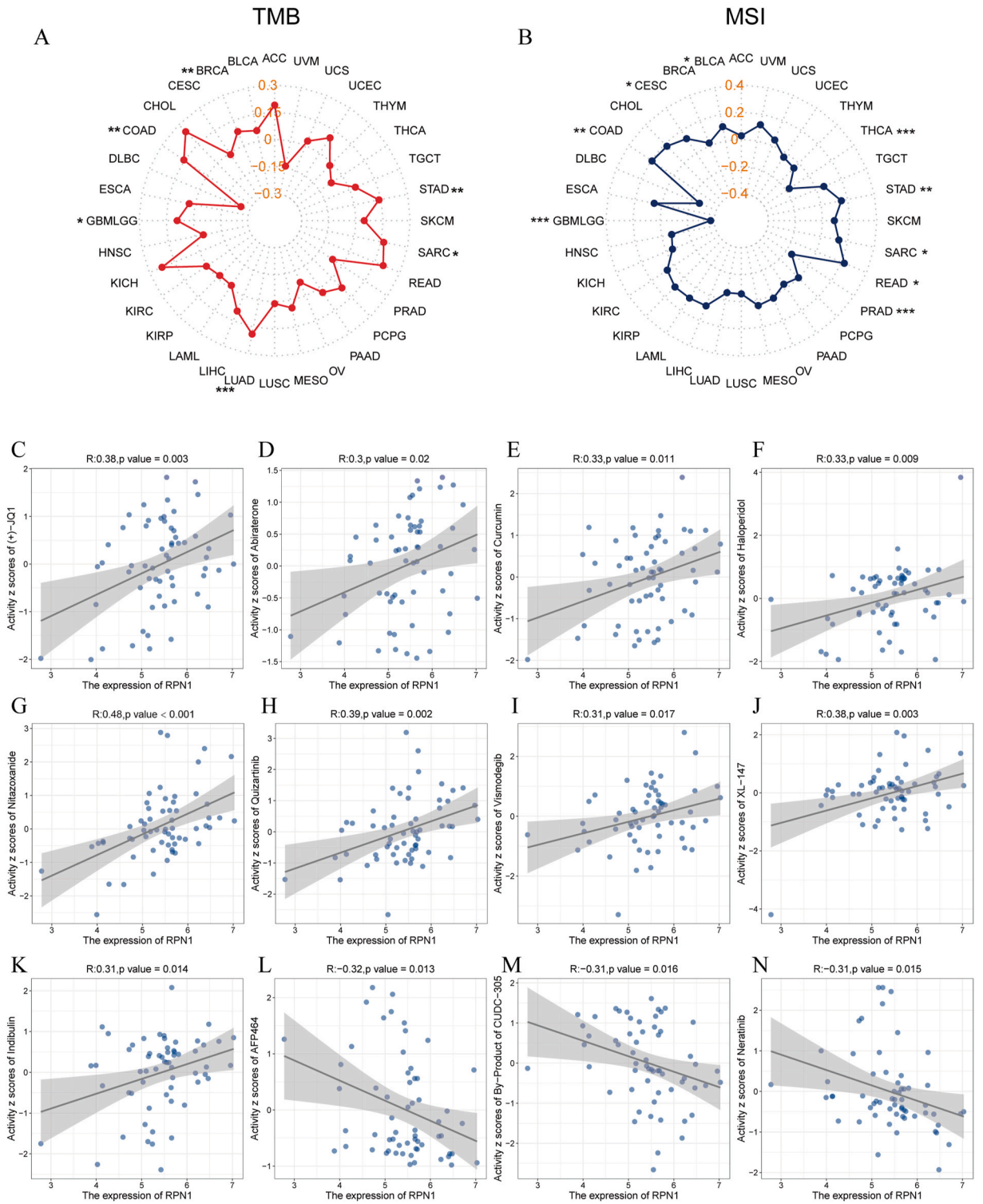
Fig. 7. (A) Radar plot of the correlation between *RPN1* expression and TMB. (B) Radar plot of the correlation between *RPN1* expression and MSI. (C–K) Drugs that increase sensitivity with elevated *RPN1* expression. (L–N) Drugs with reduced sensitivity and elevated *RPN1* expression. "*" denotes $p < 0.05$, "**" denotes $p < 0.01$, "***" denotes $p < 0.001$.
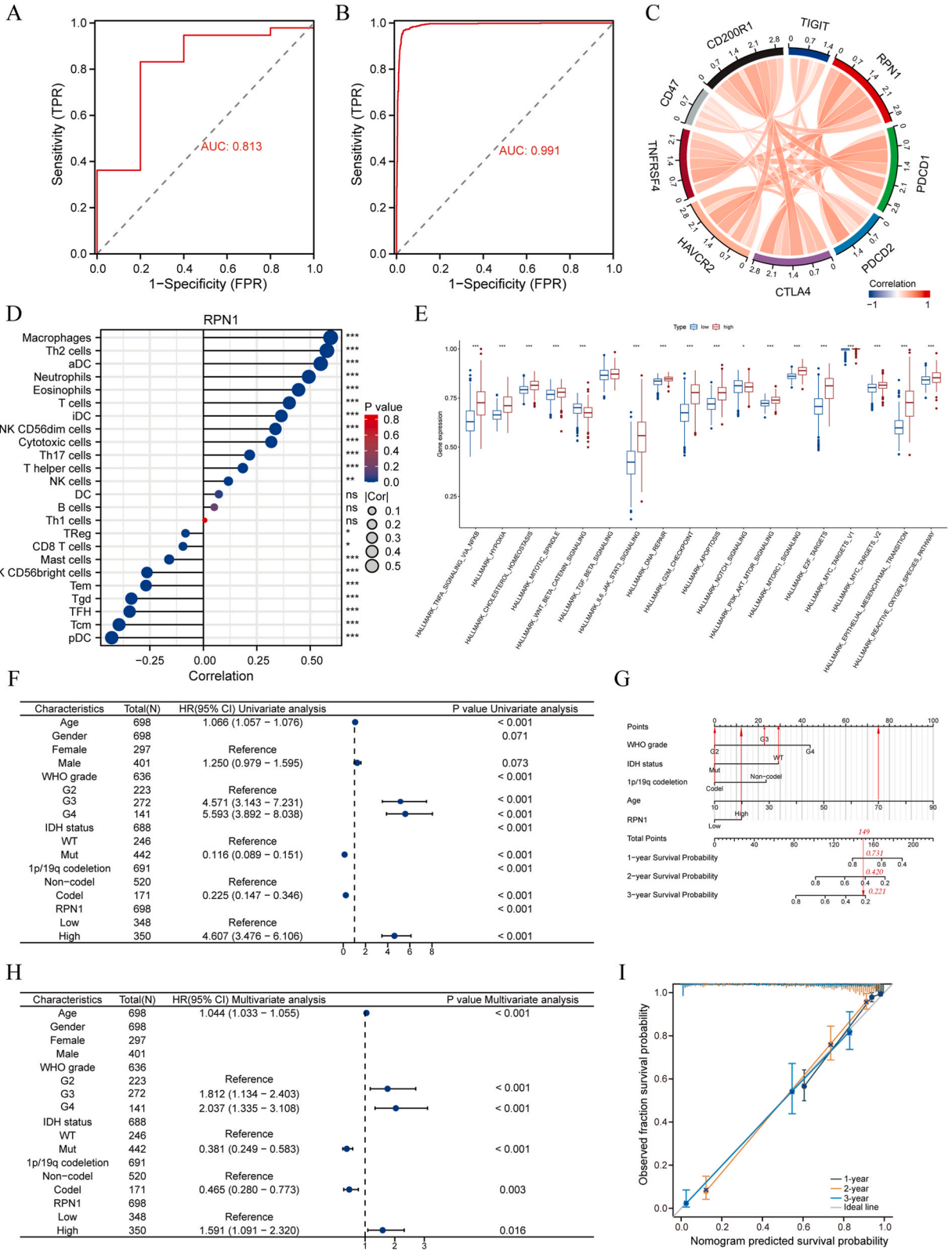
(caption on next page)

Fig. 8. (A–B) ROC curves of TCGA-GBMLGG and TCGA-GTEx. (C) Chord plot of the correlation between *RPN1* and immunosuppressive checkpoints, with a positive correlation in red and a negative correlation in blue. (D) Correlation between *RPN1* and immune cells in gliomas. (E) Correlation between *RPN1* and immune-related functions or pathways in gliomas. (F, H) Univariate and multivariate regression analyses of *RPN1* in GBMLGG. (G) A nomogram was created based on the clinical characteristics of gliomas and *RPN1*. (I) Calibration curves were established to verify the accuracy of the nomogram.

Table S3). These results confirmed the feasibility of *RPN1* as an immunotherapeutic target.

3.7. Drug sensitivity analysis of RPN1 in pan-cancer

After discussing the potential immunotherapeutic value of RPN1, we analyzed the effects of RPN1 expression on drugs. The results showed that RPN1 expression increased the sensitivity to JQ-1, abiraterone, curcumin, haloperidol, indibulin, nitazoxanide, quizartinib, vismodegib, and XL-147 (Fig. 7C–K), whereas RPN1 expression increased the resistance to AFP464, CUDC-305, and neratinib (Fig. 7L-N). Many of these drugs are used for the clinical treatment of cancer, including neratinib for breast cancer and abiraterone for prostate cancer.

3.8. Clinical value of RPN1 in gliomas

In several of the aforementioned studies, glioma samples showed significant results. We focused on examining the specific link between *RPN1* and glioma. Based on the ROC curves, in the training cohort, the area under the curve (AUC) was 0.813 (Fig. 8A), whereas in the validation cohort, the AUC was 0.991 (Fig. 8B). This result indicates that *RPN1* has a good predictive performance for gliomas. In addition, using univariate and multivariate Cox regression analyses (Fig. 8F–H), we identified *RPN1*, Age, WHO grade, IDH status, and 1p/19q co-deletion as independent prognostic factors for gliomas. Based on these factors, we constructed a nomogram to predict the 1-, 2-, and 3-year survival probabilities of patients with glioma (Fig. 8G). For instance, in a patient with glioma with a WHO
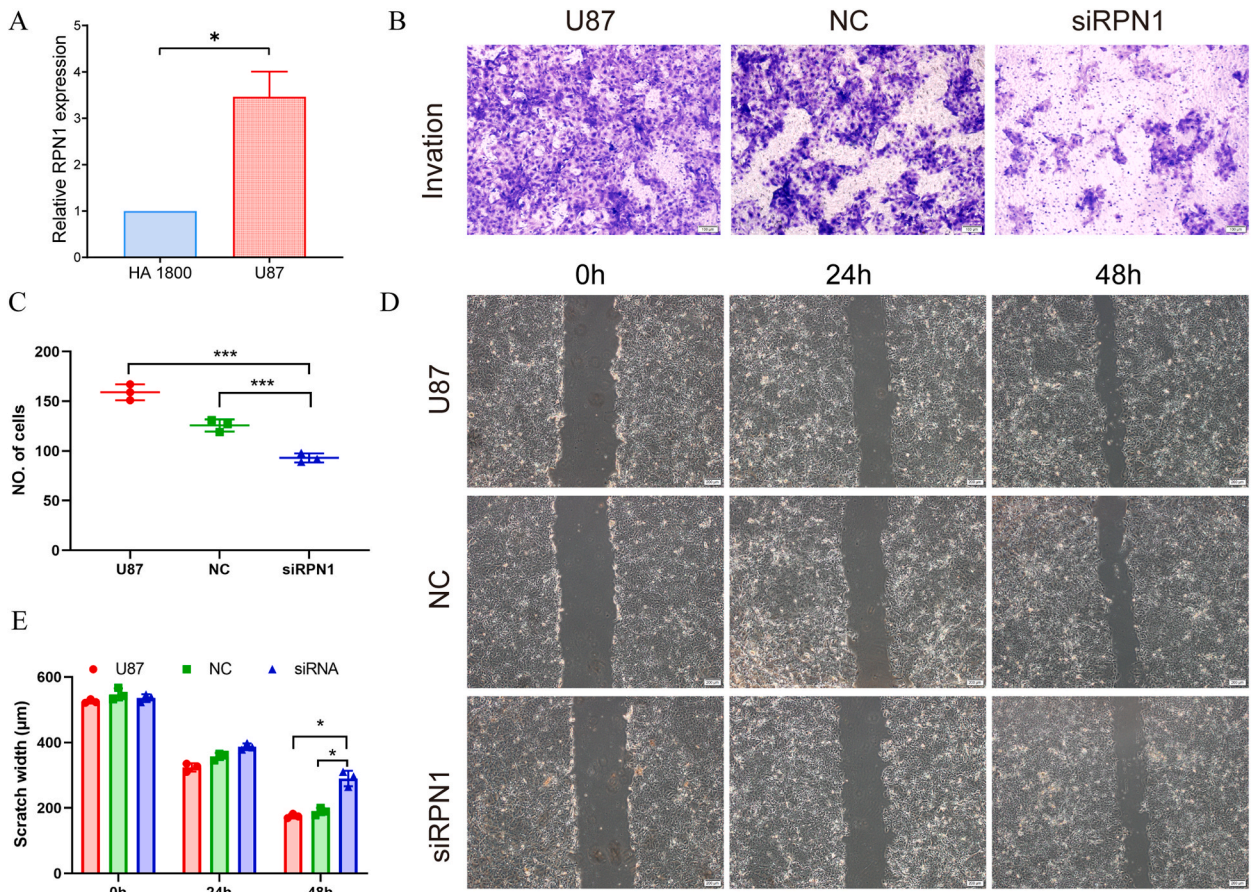
Fig. 9. (A) Results of *RPN1* expression in astrocytes and glioma cells detected using PCR. (B) Transwell assay of the three groups of cells (U87, NC, siRNA) to detect cell invasion. (C) Statistical results of the invasion assay for three groups of cells. (D) Results of the scratch assay for the three groups of cells. (E) Statistical results of the scratch assay.

grade of grade 3, the IDH status was classified as wild-type, and a 1p/19q co-deletion status was designated as Codel. The patient was 70 years old and concurrently presented with a high RPN risk score. Based on composite score calculations, the patient's total score was 149. Consequently, the anticipated 1-year survival rate for this patient was 0.731, the 2-year survival rate was 0.420, and the 3-year survival rate was 0.221. Calibration curves were constructed to assess the predictive performance of the nomograms. The ideal line represents the prediction curve, whereas the green, orange, and blue lines represent patient survival outcomes. The closer the overlap between the two, the better the predictive performance, indicating that the nomogram has a good predictive performance for patient prognosis (Fig. 8I).

3.9. Results of immune correlation analyses

Immunotherapy is widely used for the clinical treatment of various cancers. The immune checkpoint blockade is a classic approach in immunotherapy [35]. Therefore, we analyzed the correlation between *RPN1* and several ICIs using Spearman's correlation co-efficients. The results indicate that *RPN1* was positively correlated with *PDCD1*, *PDCD2*, *CTLA4*, *HAVCR2*, *TNFRSF4*, *CD47*, *CD200R1*, and *TIGIT* (Fig. 8C), suggesting that *RPN1* may serve as a potential therapeutic target for gliomas.

Furthermore, we used the ssGSEA algorithm to evaluate the infiltration levels of 24 immune cell types in gliomas. The results demonstrate that the expression of *RPN1* was correlated with the infiltration of 21 immune cell types (Fig. 8D). Specifically, it showed significant positive correlations with macrophages, Th2 cells, activated dendritic cells (aDCs), neutrophils, eosinophils, T cells, immature dendritic cells (iDCs), NK CD56dim cells, and cytotoxic cells, while exhibiting significant negative correlations with plasmacytoid dendritic cells (pDCs), central memory T cells (Tcm), T follicular helper cells (TFH), γδ T cells (Tgd), effector memory T cells (Tem), and NK CD56 bright cells ($p < 0.05$, $|cor| > 0.25$).

In the correlation analysis with hallmark gene sets, we found that the high expression group of RPN1 had higher enrichment scores in multiple gene sets (including the TNF-α Signaling via NF-κB Pathway, hypoxia, cholesterol homeostasis, mitotic spindle, IL6-JAK-STAT3 signaling pathway, DNA repair, G2/M checkpoint, apoptosis, PI3K-AKT-mTOR signaling pathway, mTORC1 signaling pathway, E2F targets, MYC targets V1, MYC targets V2, epithelial-mesenchymal transition, reactive oxygen species pathway). Conversely, in Wnt-β-catenin signaling pathway and Notch signaling pathway, the low expression group of RPN1 presented higher enrichment scores (Fig. 8E). We have elaborated on this in the Discussion section.

3.10. Results of the experimental validation

qRT-PCR results demonstrated that the expression level of *RPN1* in glioma cells (U87) was higher than that in normal human astrocytes (HA-1800) (Fig. 9A). According to the results of the transwell invasion and scratch assays, the invasion and migration abilities of the siRNA group decreased (Fig. 9B–E). In other words, after the knockdown of *RPN1* expression, glioma cell invasion, and migration abilities were significantly decreased. This result was consistent with the prognostic analysis, further confirming that high expression of *RPN1* leads to an adverse prognosis.

4. Discussion

Abnormal cell death patterns are one of the hallmarks of cancer development, and the treatment of cancer using multiple PCD modalities is a popular topic in cancer research [14,36]. Several studies have shown that disulfidptosis-related genes (DRGs) are involved in the development and progression of various cancers [36]. The ribonucleoprotein (RPN) family is an essential regulatory subunit of the proteasome that affects cellular physiological and pathological processes by regulating proteasome activity, leading to tumorigenesis [37,38]. *RPN1*, a critical gene in the RPN family associated with disulfidptosis, was investigated for its potential impact on cancer. Our observation of aberrant expression of *RPN1* in cancer and its impact on the prognosis of patients with tumors highlights its potential as a prognostic indicator of cancer. Consequently, we investigated the functional role of *RPN1* in tumors.

Immune cells in the tumor microenvironment are essential factors influencing disease progression and prognosis [39,40]. Therefore, we investigated the correlation between *RPN1* expression and immune cell infiltration in tumor tissues. Notably, *RPN1* was positively correlated with MDSC, neutrophils, and macrophages and negatively correlated with CD8+T cells and HSCs. These findings suggest that *RPN1* affects tumor development and patient prognosis by suppressing the activity of antitumor immune cells and regulating the infiltration of various immune cells. These results indicate the potential significance of *RPN1* in tumor immune regulation, offering a novel perspective for precision therapy. However, different tumor or immune-related tools can lead to errors in their correlation results. Therefore, it is imperative to select specific algorithms for analysis based on the tumor type and analysis target.

Numerous studies have identified genetic modifications that are closely associated with cancer development and progression [41]. Therefore, we explored the potential link between *RPN1* and cancer at the genetic level. Additionally, gene alterations can affect the approach and effectiveness of cancer treatment [42,43]. We found that the most predominant form of *RPN1* mutation status in cancer was amplification, and amplification of the gene should be considered a hallmark of carcinogenesis [44]. In cancer cells, *RPN1* promoter methylation tends to be reduced, which can lead to disturbed gene expression and genomic instability [45,46]. Interestingly, the mutation in *RPN1* significantly increased the mutation rates of *SULT1D1P*, *LRRTM4-AS1*, *LINC01851*, *SNAR-H*, *LINC01565*, *DNAJB8*, *PLXND1*, *DNAJB8-AS1*, *CFAP92*, and *PLXNA1*. This indicates that *RPN1* mutations may lead to instability in other genes that affect tumor development. In addition, mutations in multiple genes may have synergistic effects, leading to complex tumor characteristics. The simultaneous increase in mutation rates across various genes implies their potential involvement in shared signaling routes or biological activities. These results provide a deeper understanding of the effects of mutations in the *RPN1* on tumorigenesis and

growth. This discovery prompted additional investigations into the correlations among *RPN1*, TMB, and MSI.

Early studies have shown that MSI levels help predict immune responses in gastric and colorectal cancers and guide immunotherapy in patients with cancer [47,48]. TMB has also been suggested as a potential immunotherapy target, and high TMB values can enhance the immune response and improve the survival rates of treated patients [49]. According to our findings, there was a significant positive correlation between the expression of *RPN1* and TMB in tumors, such as GBMLGG, LUAD, COAD, BRCA, SARC, and STAD. Additionally, in CESC, COAD, SARC, STAD, READ, and BLCA, a significant positive correlation existed between the expression of *RPN1* and MSI. In GBMLGG, PRAD, and THCA, the expression of *RPN1* was negatively correlated with MSI levels. Therefore, these results are important. They confirmed the importance of *RPN1* in different tumor types and revealed its association with tumor immune characteristics. Second, these findings provide new evidence for utilizing *RPN1* as a potential immunotherapy target, especially for tumors with high TMB or MSI positivity. Subsequently, we focused on *RPN1*'s responsiveness to anticancer drugs.

Therefore, we investigated the sensitivity of *RPN1* to a variety of drugs, and the results confirmed that the expression of *RPN1* was positively correlated with sensitivity to various drugs, such as JQ-1, abiraterone, curcumin, haloperidol, nitazoxanide, quizartinib, XL-147, indibulin, and vismodegib. Conversely, increased *RPN1* expression increased resistance to AFP464, CUDC-305, and neratinib and set the stage for the clinical use of these drugs. Neratinib has been highlighted in previous studies as an instructive agent for the design of glioma kinase inhibitors [50]. Focusing on changes in drug resistance is valuable for subsequent drug activity in antitumor therapy.

In the pan-cancer studies described above, gliomas always showed significant results, and *RPN1* was highly expressed in gliomas, leading to a poor prognosis. Therefore, we investigated the relationship between *RPN1* and gliomas. The AUCs of the ROC curves of the two datasets (TCGA-GBMLGG and TCGA-GTEx) were all >0.8. This demonstrated the excellent diagnostic performance of PRN1 in gliomas. Univariate and multivariate Cox regression analyses indicated that *RPN1* is an independent prognostic factor for gliomas. A nomogram constructed based on *RPN1* and multiple clinical characteristics (age, WHO grade, IDH status, and 1p/19q codeletion) also showed excellent prognostic predictive performance. These findings suggest that *RPN1* is a potential immune biomarker for gliomas. Therefore, we analyzed the correlation between *RPN1* and gliomas.

First, we analyzed the relationship between *RPN1* expression and various ICIs including *PDCD1*, *PDCD2*, *CTLA4*, *HAVCR2*, *TNFRSF4*, *CD47*, *CD200R1*, and *TIGIT*. This yielded an intriguing result, as these ICIs play crucial roles in tumor therapy [35,51]. And *RPN1* showed a highly positive correlation with these ICIs. Therefore, it is reasonable to speculate that the function of *RPN1* is similar to those of these targets. This finding is superior to those of previous studies, including those related to glioma based on ferroptosis and cuproptosis [52,53].

Second, immunotherapeutic modulation of the glioma microenvironment has been identified as an effective intervention [54]. Using the ssGSEA algorithm, we determined the correlation between *RPN1* and immune cells within gliomas. We observed a positive correlation among *RPN1* and macrophages, Th2 cells, and T cells, suggesting its potential positive role in triggering antitumor immune responses. This reflects the promotional effect of *RPN1* on immune cell activity, which may be produced by enhancing the phagocytosis of macrophages, stimulating Th2 immune responses, and increasing T cell activity. However, *RPN1* was negatively correlated with pDC, indicating that high expression of *RPN1* may suppress the immune response to viral infections. Additionally, its infiltration into Tcm, TFH, Tgd, Tem, and NK CD56dim cells showed a negative correlation, suggesting that high expression of *RPN1* may also inhibit the migration or function of these immune cells. These findings are important for a deeper understanding of immune regulatory mechanisms and the development of therapeutic strategies for related diseases. The intricate role of *RPN1* in the immune microenvironment makes it a worthwhile research target and a potential focal point for future immunotherapies. Further exploration of the interaction between *RPN1* and immune cells and the molecular mechanisms of immune evasion will provide profound insights for developing more precise immunotherapeutic strategies.

Finally, we found that *RPN1* expression was closely associated with various immune-related biological functions or signaling pathways. Notably, *RPN1* was positively correlated with hypoxia-related gene sets and IL6-JAK-STAT3 signaling pathway-related gene sets. Hypoxia in the tumor microenvironment leads to increased tumor cell invasiveness and resistance to chemotherapy and radiotherapy [55]. In contrast, the IL6-JAK-STAT3 signaling pathway has been targeted for the treatment of glioma [56]. Several other immune-related gene sets (mTORC1 signaling pathway, Wnt/β-catenin signaling pathway, and DNA repair) are closely associated with cancer progression and treatment. These results suggest that *RPN1* may regulate tumor initiation and progression through these pathways, providing novel insights into the treatment of gliomas.

However, this study has some limitations. The analyses lacked depth and required a more comprehensive sample size for confirmation. Although we used cellular experiments for validation, further functional and animal experiments are required to validate our results.

In summary, this paper investigated the expression levels and mutational status of RPN1 in pan-cancer, as well as its impact on the prognosis, immune infiltration, and drug sensitivity of various cancers. These studies confirm that RPN1 may influence the occurrence, development, and prognosis of multiple cancers by affecting the immune microenvironment, thus providing new insights into cancer therapy. Additionally, the close correlation of RPN1 with the treatment and prognosis of gliomas suggests its potential as a promising target for glioma therapy.

Funding

Ethics approval and consent to participate

The patient data in this work is from publicly available patients consent to a complete data set without ethical approval.

Data availability

The gene expression matrix and clinical data for pan-cancer analysis were sourced from The Cancer Genome Atlas (TCGA) database and The Genotype-Tissue Expression (GTEx) database. All data were downloaded in August 2022.

Consent for publication

Not applicable.

CRediT authorship contribution statement

Yan Zong: Writing – original draft, Visualization, Validation, Investigation, Funding acquisition, Formal analysis, Data curation, Conceptualization. **Ankang Zhu:** Writing – review & editing, Visualization, Validation, Supervision, Formal analysis, Data curation, Conceptualization. **Peipei Liu:** Writing – review & editing, Supervision, Funding acquisition, Conceptualization. **Peiji Fu:** Writing – original draft, Resources, Project administration, Methodology, Data curation. **Yinuo Li:** Writing – original draft, Visualization, Validation, Software, Formal analysis, Conceptualization. **Shuai Chen:** Writing – original draft, Visualization, Validation, Software, Resources, Project administration. **Xingcai Gao:** Writing – review & editing, Validation, Methodology.

Declaration of competing interest

The authors declare that they have no known competing financial interests or personal relationships that could have appeared to influence the work reported in this paper.

List of abbreviations

TCGA	The Cancer Genome Atlas
GTEx	Genotype-Tissue Expression
GO	Genetic Oncology
BP	Biological Pathways
CC	Cellular Component
MF	Molecular Function
CGGA	Chinese Glioma Genome Atlas
GBMLGG	Glioma
HR	Hazard Ratio
IHC	Immunohistochemical
ROC	Receiver Operating Characteristic
HSCs	Hematopoietic Stem Cells
MDSC	Myeloid-derived Suppressor Cells
CAF	Cancer-Associated Fibroblasts
mDCs	Myeloid Dendritic Cells
ICI	Immune Checkpoint Inhibitor
DC	Dendritic Cell
DRGS	Disulfidptosis-related Genes
ssGSEA	single-sample Gene Set Enrichment Analysis
HPA	Human Protein Atlas
KEGG	Kyoto Encyclopedia of Genes and Genomes
MSI	Microsatellite Instability
OS	Overall survival
TMB	Tumor Mutation burden
Treg	Regulatory T cell
AUC	Area Under Curve
PCD	Programmed Cell Death
FBS	Fetal Bovine Serum

NK	Natural Killer Cells
Tcm	Central Memory T Cells
pDC	Plasmacytoid Dendritic Cells
TFH	T Follicular Helper Cells
Tgd	$\gamma\delta$ T cells
TEM	Effector memory T cells
aDCs	Activated dendritic cells
iDCs	Immature dendritic cells

Appendix A. Supplementary data

Supplementary data to this article can be found online at https://doi.org/10.1016/j.heliyon.2024.e31875.

References

[1] R.L. Siegel, et al., Cancer statistics, 2022, CA A Cancer J. Clin. 72 (1) (2022) 7–33.
[2] W. Cao, et al., Changing profiles of cancer burden worldwide and in China: a secondary analysis of the global cancer statistics 2020, Chin. Med. J. 134 (7) (2021) 783–791.
[3] P.A. Jeggo, L.H. Pearl, A.M. Carr, DNA repair, genome stability and cancer: a historical perspective, Nat. Rev. Cancer 16 (1) (2016) 35–42.
[4] N.J. Mullen, P.K. Singh, Nucleotide metabolism: a pan-cancer metabolic dependency, Nat. Rev. Cancer 23 (5) (2023) 275–294.
[5] J. Choi, et al., G2Vec: distributed gene representations for identification of cancer prognostic genes, Sci. Rep. 8 (1) (2018) 13729.
[6] M. Kim, I. Oh, J. Ahn, An improved method for prediction of cancer prognosis by network learning, Genes 9 (10) (2018).
[7] L. Xu, et al., Pan-cancer analysis identifies CHD5 as a potential biomarker for glioma, Int. J. Mol. Sci. 23 (15) (2022).
[8] Y. He, et al., Pan-cancer analysis reveals NUP37 as a prognostic biomarker correlated with the immunosuppressive microenvironment in glioma, Aging (Albany NY) 14 (2) (2022) 1033–1047.
[9] Q.T. Ostrom, et al., The epidemiology of glioma in adults: a "state of the science" review, Neuro Oncol. 16 (7) (2014) 896–913.
[10] K. Yang, et al., Glioma targeted therapy: insight into future of molecular approaches, Mol. Cancer 21 (1) (2022) 39.
[11] A. Strasser, D.L. Vaux, Cell death in the origin and treatment of cancer, Mol. Cell 78 (6) (2020) 1045–1054.
[12] X. Jiang, B.R. Stockwell, M. Conrad, Ferroptosis: mechanisms, biology and role in disease, Nat. Rev. Mol. Cell Biol. 22 (4) (2021) 266–282.
[13] D. Tang, et al., Ferroptosis: molecular mechanisms and health implications, Cell Res. 31 (2) (2021) 107–125.
[14] T. Zheng, et al., Disulfidptosis: a new form of programmed cell death, J. Exp. Clin. Cancer Res. 42 (1) (2023) 137.
[15] X. Liu, et al., Actin cytoskeleton vulnerability to disulfide stress mediates disulfidptosis, Nat. Cell Biol. 25 (3) (2023) 404–414.
[16] S. Zhao, et al., Crosstalk of disulfidptosis-related subtypes, establishment of a prognostic signature and immune infiltration characteristics in bladder cancer based on a machine learning survival framework, Front. Endocrinol. 14 (2023) 1180404.
[17] C. Zheng, et al., Circ-SNX27 sponging miR-375/RPN1 axis contributes to hepatocellular carcinoma progression, KOREAN J. PHYSIOL. PHARMACOL. 27 (4) (2023) 333–344.
[18] C. Jiang, et al., Prognosis prediction of disulfidptosis-related genes in bladder cancer and a comprehensive analysis of immunotherapy, Crit. Rev. Eukaryot. Gene Expr. 33 (6) (2023) 73–86.
[19] T. Li, et al., TIMER2.0 for analysis of tumor-infiltrating immune cells, Nucleic Acids Res. 48 (W1) (2020) W509–W514.
[20] K. Colwill, G. Renewable Protein Binder Working, S. Graslund, A roadmap to generate renewable protein binders to the human proteome, Nat. Methods 8 (7) (2011) 551–558.
[21] T. Emura, S. Matsui, H.Y. Chen, compound.Cox: univariate feature selection and compound covariate for predicting survival, Comput. Methods Progr. Biomed. 168 (2019) 21–37.
[22] A. Lanczky, B. Gyorffy, Web-based survival analysis tool tailored for medical research (KMplot): development and implementation, J. Med. Internet Res. 23 (7) (2021) e27633.
[23] T. Li, et al., TIMER: a web server for comprehensive analysis of tumor-infiltrating immune cells, Cancer Res. 77 (21) (2017) e108–e110.
[24] Z. Tang, et al., GEPIA: a web server for cancer and normal gene expression profiling and interactive analyses, Nucleic Acids Res. 45 (W1) (2017) W98–W102.
[25] D.S. Chandrashekar, et al., UALCAN: an update to the integrated cancer data analysis platform, Neoplasia 25 (2022) 18–27.
[26] J. Gao, et al., Integrative analysis of complex cancer genomics and clinical profiles using the cBioPortal, Sci. Signal. 6 (269) (2013) pl1.
[27] R. Bonneville, et al., Landscape of microsatellite instability across 39 cancer types, JCO Precis Oncol. 2017 (2017).
[28] U.T. Shankavaram, et al., CellMiner: a relational database and query tool for the NCI-60 cancer cell lines, BMC Genom. 10 (2009) 277.
[29] V.P. Balachandran, et al., Nomograms in oncology: more than meets the eye, Lancet Oncol. 16 (4) (2015) e173–e180.
[30] B.I. Bagus, Autologous natural killer cells as a promising immunotherapy for locally advanced colon adenocarcinoma: three years follow-up of resectable case, Cancer Rep. (Hoboken) 6 (9) (2023) e1866.
[31] X. Dai, et al., Methylation multiplicity and its clinical values in cancer, Expet Rev. Mol. Med. 23 (2021) e2.
[32] M. Palmeri, et al., Real-world application of tumor mutational burden-high (TMB-high) and microsatellite instability (MSI) confirms their utility as immunotherapy biomarkers, ESMO Open 7 (1) (2022) 100336.
[33] A. Rizzo, A.D. Ricci, G. Brandi, PD-L1, TMB, MSI, and other predictors of response to immune checkpoint inhibitors in biliary tract cancer, Cancers 13 (3) (2021).
[34] E. Karamitopoulou, et al., High tumor mutational burden (TMB) identifies a microsatellite stable pancreatic cancer subset with prolonged survival and strong anti-tumor immunity, Eur. J. Cancer 169 (2022) 64–73.
[35] P. Darvin, et al., Immune checkpoint inhibitors: recent progress and potential biomarkers, Exp. Mol. Med. 50 (12) (2018) 1–11.
[36] P. Zheng, et al., Disulfidptosis: a new target for metabolic cancer therapy, J. Exp. Clin. Cancer Res. 42 (1) (2023) 103.
[37] W. Zheng, et al., RPNs levels are prognostic and diagnostic markers for hepatocellular carcinoma, J Oncol 2022 (2022) 7270541.
[38] A.M. Weissman, Themes and variations on ubiquitylation, Nat. Rev. Mol. Cell Biol. 2 (3) (2001) 169–178.
[39] T.F. Gajewski, H. Schreiber, Y.X. Fu, Innate and adaptive immune cells in the tumor microenvironment, Nat. Immunol. 14 (10) (2013) 1014–1022.
[40] X. Mao, et al., Crosstalk between cancer-associated fibroblasts and immune cells in the tumor microenvironment: new findings and future perspectives, Mol. Cancer 20 (1) (2021) 131.
[41] M. Mina, et al., Conditional selection of genomic alterations dictates cancer evolution and oncogenic dependencies, Cancer Cell 32 (2) (2017) 155–168 e6.
[42] M.F. Berger, E.R. Mardis, The emerging clinical relevance of genomics in cancer medicine, Nat. Rev. Clin. Oncol. 15 (6) (2018) 353–365.
[43] P.T.C. Group, et al., Genomic basis for RNA alterations in cancer, Nature 578 (7793) (2020) 129–136.
[44] M. Macheret, T.D. Halazonetis, DNA replication stress as a hallmark of cancer, Annu. Rev. Pathol. 10 (2015) 425–448.

[45] F.R. Traube, T. Carell, The chemistries and consequences of DNA and RNA methylation and demethylation, RNA Biol. 14 (9) (2017) 1099–1107.

[46] A.M. Mahmoud, M.M. Ali, Methyl donor micronutrients that modify DNA methylation and cancer outcome, Nutrients 11 (3) (2019).

[47] A. Lin, J. Zhang, P. Luo, Crosstalk between the MSI status and tumor microenvironment in colorectal cancer, Front. Immunol. 11 (2020) 2039.

[48] E. Puliga, et al., Microsatellite instability in Gastric Cancer: between lights and shadows, Cancer Treat Rev. 95 (2021) 102175.

[49] R.M. Samstein, et al., Tumor mutational load predicts survival after immunotherapy across multiple cancer types, Nat. Genet. 51 (2) (2019) 202–206.

[50] C.P. Tang, et al., GCN2 kinase activation by ATP-competitive kinase inhibitors, Nat. Chem. Biol. 18 (2) (2022) 207–215.

[51] D.M. Pardoll, The blockade of immune checkpoints in cancer immunotherapy, Nat. Rev. Cancer 12 (4) (2012) 252–264.

[52] W. Wang, et al., Identifies microtubule-binding protein CSPP1 as a novel cancer biomarker associated with ferroptosis and tumor microenvironment, Comput. Struct. Biotechnol. J. 20 (2022) 3322–3335.

[53] Z. Wu, et al., Identification of cuproptosis-related subtypes and the development of a prognostic model in glioma, Front. Genet. 14 (2023) 1124439.

[54] D.F. Quail, et al., The tumor microenvironment underlies acquired resistance to CSF-1R inhibition in gliomas, Science 352 (6288) (2016) aad3018.

[55] V. Amberger-Murphy, Hypoxia helps glioma to fight therapy, Curr. Cancer Drug Targets 9 (3) (2009) 381–390.

[56] W. Fu, et al., Roles of STAT3 in the pathogenesis and treatment of glioblastoma, Front. Cell Dev. Biol. 11 (2023) 1098482.